The Restricted 3-Body Problem

John Bremseth and John Grasel

12/10/2010

Abstract

Though the 3-body problem is difficult to solve, it can be modeled if one mass is so small that its effect on the other two bodies is negligible. This situation occurs in real-life where a binary star system, such as the one formed by the gravitationally bound stars α Centauri A and B, traps a low mass planet. The computed model correctly predicted elliptical orbits for the stars, as well as S-type and P-type orbits for a planet. This paper analyzes the range of stable planetary orbits and investigates the impact of a binary star on a distant planet relative to a single star of equal mass, and the effect such a planet would feel orbiting around one star due to the other star. While no planets have been observed in the α Centauri system, astronomers use computer models not dissimilar to this to predict likely orbits and inform their observations.

A binary star is a star system composed of two stars trapped in elliptical orbits around their shared center of mass by each other's gravity. The larger of the two stars is called the primary star, and the smaller is called the secondary star. By analyzing a system where the two binary stars are massive compared to the planet, the project is confined to a restricted 3-body problem. This allows for the independent calculation of the equations of motion of the binary stars before calculating the motion of the planet.

1 2-Body Equations of Motion

$\boldsymbol{r_1}$ and $\boldsymbol{r_2}$ are defined as the position of the binary stars with mass M_1 and M_2 as shown in Fig. 1. The Lagrangian of the two-body problem is

$$L = \frac{1}{2}M_1\dot{\boldsymbol{r}}_1^2 + \frac{1}{2}M_1\dot{\boldsymbol{r}}_2^2 - V(|\boldsymbol{r}_1 - \boldsymbol{r}_2|) \tag{1}$$

Where V($|\boldsymbol{r}_1 - \boldsymbol{r}_2|$) is the gravitational potential of the two stars. If $\boldsymbol{r} \equiv \boldsymbol{r}_1 - \boldsymbol{r}_2$, and the center of mass is chosen to coincide with the origin so that $M_1|\boldsymbol{r}_1| + M_2|\boldsymbol{r}_2| = 0$, then:

$$\boldsymbol{r}_1 = \frac{M_2\boldsymbol{r}}{M_1 + M_2}, \boldsymbol{r}_2 = \frac{-M_1\boldsymbol{r}}{M_1 + M_2} \tag{2}$$

The reduced mass of the binary orbit is defined to be

$$\mu = \frac{M_1 M_2}{M_1 + M_2} \tag{3}$$

simplifying the Lagrangian to

$$\mathscr{L} = \frac{1}{2}\mu \dot{\boldsymbol{r}}^2 - V(\boldsymbol{r}) \tag{4}$$

The binary star system has thus been reduced to a single body of mass μ orbiting a fixed point, the center of mass of the binary system, at radius r and angle θ as shown in Fig. 2. If r is defined as $|\boldsymbol{r}|$ and θ is defined as the angle between M_1 and the semi-major axis as shown in Fig. 1, then the

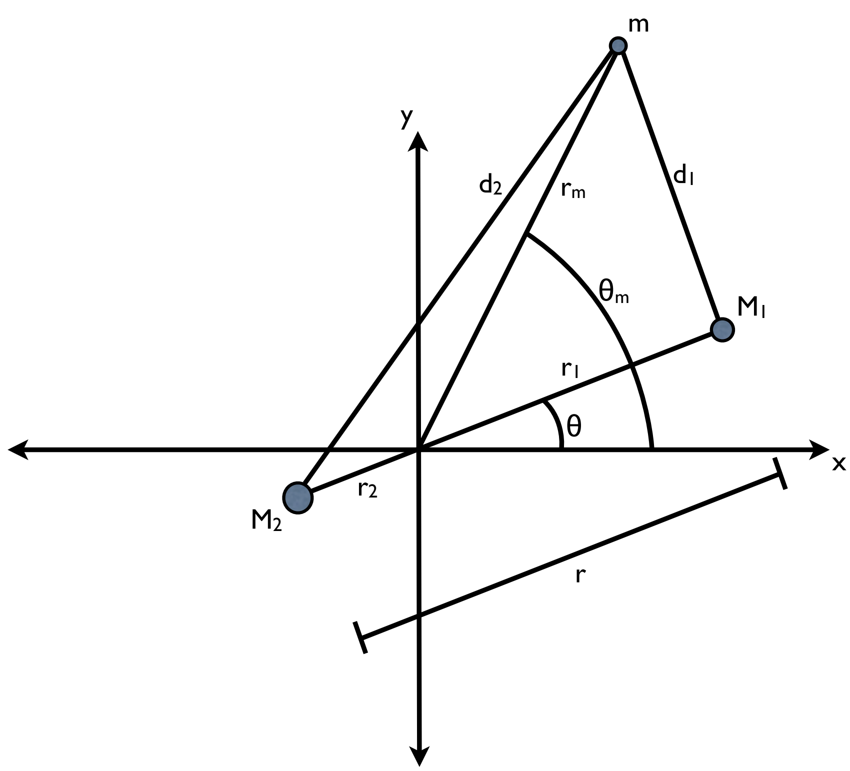

Figure 1: **Setup** - System diagram for modeling the motion of the binary stars (M_1 and M_2) and the planet (m). To simplify the diagrammed 3-body problem, m is approximated to be very small compared to M_1 and M_2. Thus, the motion of the stars can be calculated first (the 2-body problem) and the motion of the planet can be added in later (the restricted 3-body problem). The origin represents the center of mass of the binary star system.

kinetic energy of the system, the first term of the Lagrangian, is described as

$$T = \frac{1}{2}\mu\left(\dot{r}^2 + r^2\dot{\theta}^2\right) \tag{5}$$

The constant for gravitational attraction is given by $k = GM_1M_2$. Gravitational force is governed by an inverse square law, so its potential is inversely proportional to separation $\boldsymbol{r}$. Thus, the potential energy, the second term on the Lagrangian, is described by

$$V(r) = -\frac{k}{r} \tag{6}$$

so the Lagrangian can be written

$$\mathscr{L} = \frac{\mu}{2}\left(\dot{r}^2 + r^2\dot{\theta}^2\right) + \frac{k}{r} \tag{7}$$

There is no explicit time dependence in the Lagrangian, so the Hamiltonian is conserved. In addition, the equations of transformation between polar and Cartesian coordinates contain no time dependence the Hamiltonian is equal to the energy. Lagrange's equation for the system with respect to θ is

$$\frac{d}{dt}\left(\frac{\partial \mathscr{L}}{\partial \dot{\theta}}\right) - \frac{\partial \mathscr{L}}{\partial \theta} = 0 = \frac{d}{dt}\left(\mu r^2\dot{\theta}\right) \tag{8}$$

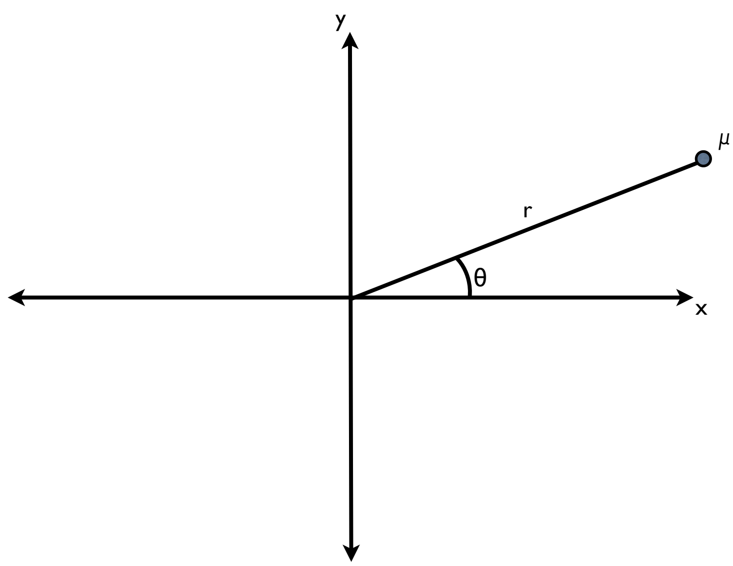

Figure 2: **Reduced Mass** - The binary star system shown in Fig. 1 is dynamically equivalent to a mass of μ orbiting a fixed object of mass $M_1 + M_2$ at radius r. Solving this simplified system imparts direct knowledge of the motions of both stars.

Eq. (8) is a statement of conservation of angular momentum, L, defined as

$$L \equiv \mu r^2 \dot{\theta} \tag{9}$$

From here, Lagrange's equations could be calculated with respect to r, and the product, two differential equations, could be numerically solved. However, due to conservation of linear and angular momentum, solving for θ as a function of time defines the binary system. Thus two differential equations would be redundant, and reducing the system to only one speeds computational time and simplifies the system. For this, radial dependence within the differential equation for θ must be removed. To accomplish this, the system's energy

$$E = T + V = \frac{\mu}{2}\left(\dot{r}^2 + r^2\dot{\theta}^2\right) - \frac{k}{r} = \frac{\mu}{2}\left(\dot{r}^2 + r^2\frac{L^2}{\mu^2 r^4}\right) - \frac{k}{r} = \frac{\mu}{2}\left(\dot{r}^2 + \frac{L^2}{\mu^2 r^2}\right) - \frac{k}{r} \tag{10}$$

is used. Solving Eq. (10) for $\dot{r}^2$ yields,

$$\dot{r}^2 = \frac{2}{\mu}\left(E - \left(\frac{L^2}{2\mu r^2} - \frac{k}{r}\right)\right) \tag{11}$$

and substituting in Eq. (9) and Eq. (11), the relation

$$\frac{dr}{d\theta} = \frac{\dot{r}}{\dot{\theta}} = \frac{\sqrt{\frac{2}{\mu}\left(E - \left(\frac{L^2}{2\mu r^2} - \frac{k}{r}\right)\right)}}{L/\mu r^2} \tag{12}$$

is formed. Changing variables from $r = 1/u$; making the appropriate substitutions and defining $\dot{u}$ and $\ddot{u}$ as derivatives of u with respect to θ, the above equation of motion becomes

$$\frac{du}{d\theta} = -\frac{\mu}{L}\sqrt{\frac{2}{\mu}\left(E - \left(\frac{L^2 u^2}{2\mu} - ku\right)\right)} \tag{13}$$

Squaring both sides and differentiating with respect to θ,

$$2\dot{u}\ddot{u} = -\frac{2\mu}{L^2}\left(\frac{dE}{d\theta} - \frac{L^2 u^2}{2\mu}\left(2u\dot{u}\right) + k\dot{u}\right) \tag{14}$$

where the system's rotational symmetry guarantees that $\frac{dE}{d\theta}$ is zero. The equation for the inverse radius with no explicit θ dependence is thus

$$\ddot{u} + u = \frac{k\mu}{L^2} \tag{15}$$

Defining $\alpha = L^2/\mu k$ and $\epsilon = \sqrt{1 + 2EL^2/\mu k^2}$, the solution to Eq. (15) is

$$\frac{\alpha}{r} = 1 + \epsilon\cos(\theta) \tag{16}$$

Solving Eq. (16) for r and substituting into Eq. (9) yields the final differential equation for θ:

$$\dot{\theta} = \frac{L\,(1 + \epsilon\cos(\theta))^2}{\mu\alpha^2} \tag{17}$$

Eq. (17) can be numerically integrated to yield $\theta(t)$, giving knowledge of the angular positions of both stars. Because θ is defined as the angle to the first star, and the angle to the second star is just $\theta + \pi$. These results can be substituted into Eq. (16) to obtain a numerical solution for $r(t)$. The radii of stars 1 and 2 can be found from the center-of-mass relation in Eq. (2). The actual constants of the α Centauri system are used; M_1 and M_2 are 1.1 and 0.85 solar masses respectively, and the eccentricity of the orbit ϵ is 0.52. These constants determine the initial radii. The initial θ in the simulations is 0 unless otherwise specified, defining the X axis in figure one to be the semi-major axis of the binary orbit.

2 3-Body Equations of Motion

Those two equations, however, only describe the two stars of the binary α Centauri. The process can be repeated for the planet. r_m is defined as the distance between the center of mass of the binary stars and the planet, and m as the planet mass, which is insignificant compared to the stars' masses. θ_m is defined as the angle between the reference angle and the planet, as shown in Fig. 1. Finally, the distances between the planet and each star, d, are defined as:

$$d_1 = \sqrt{r_m^2 + r_1^2 - 2r_m r_1\cos(\theta_m - \theta)} \tag{18}$$

$$d_2 = \sqrt{r_m^2 + r_2^2 + 2r_m r_2\cos(\theta_m - \theta)} \tag{19}$$

where the factor of π in d_2 is accounted for with a sign difference. The kinetic energy for the planet is described by

$$T = \frac{m}{2}(\dot{r}_m^2 + r_m^2\dot{\theta}_m^2) \tag{20}$$

and the potential energy is described by

$$V = -\frac{GM_1 m}{d_1} - \frac{GM_2 m}{d_2} \tag{21}$$

yielding a Lagrangian of:

$$\mathscr{L} = \frac{m}{2}(\dot{r}_m^2 + r_m^2\dot{\theta}_m^2) + \frac{GM_1 m}{d_1} + \frac{GM_2 m}{d_2} \tag{22}$$

Solving the Lagrangian with respect to r_m and θ_m yield the following equations of motion.

$$\ddot{r}_m = r_m\dot{\theta}_m^2 - GM_1\frac{r_m - r_1\cos(\theta_m - \theta)}{d_1^{3/2}} - GM_2\frac{r_m + r_2\cos(\theta_m - \theta)}{d_2^{3/2}} \tag{23}$$

$$2r_m\dot{r}_m\dot{\theta} + r_m^2\ddot{\theta}_m = -GM_1\frac{r_m r_1\sin(\theta_m - \theta)}{d_1^{3/2}} + GM_2\frac{r_m r_2\sin(\theta_m - \theta)}{d_2^{3/2}} \tag{24}$$

These equations are numerically solvable using Mathematica. The planet's initial position and velocity (r, $\dot{r}$, θ, and $\dot{\theta}$) are defined relative to the center of mass of the binary system. These are specified on the plots only if nonzero.

3 Results

As predicted, the simulation of the binary system shows the binary stars completing their orbits with a period of 80 years as seen in Fig. 3. The massive star orbits more closely to the center of mass than the lighter star, and the stars are observed moving more rapidly near the barycenter, the binary stars' center of mass, of the system. The graphics depict the passage of time through the coloring of the orbit: purple represents the beginning of the simulation, and the color gradient represents passage of time. Because

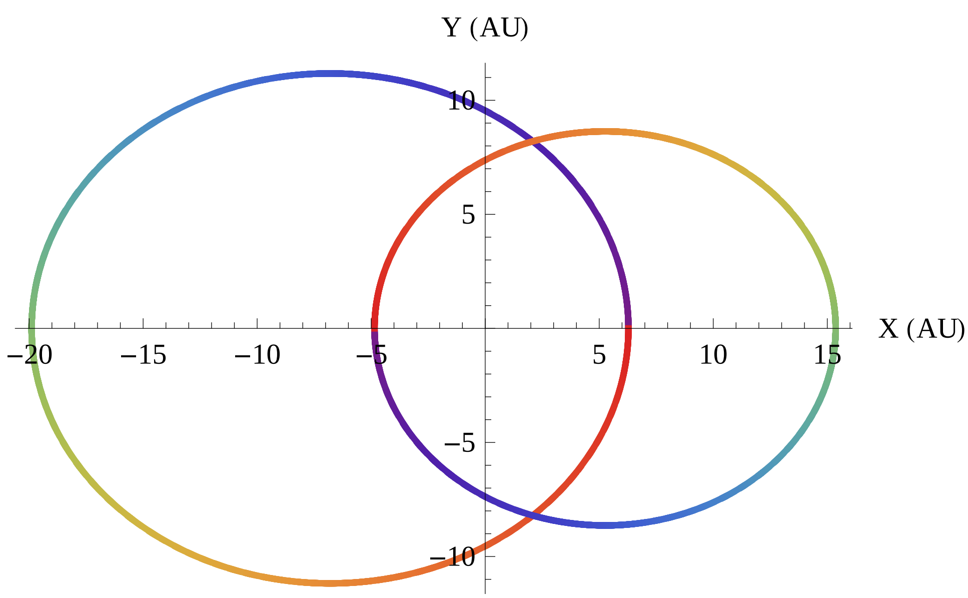

Figure 3: **Binary Star System** - The two stars in the α Centauri system orbit each other elliptically with a period of 80 years. The coloring of the system depicts the passage of time which evolves from purple to red. For this and following simulations, the stars begin their orbits at Perigee.

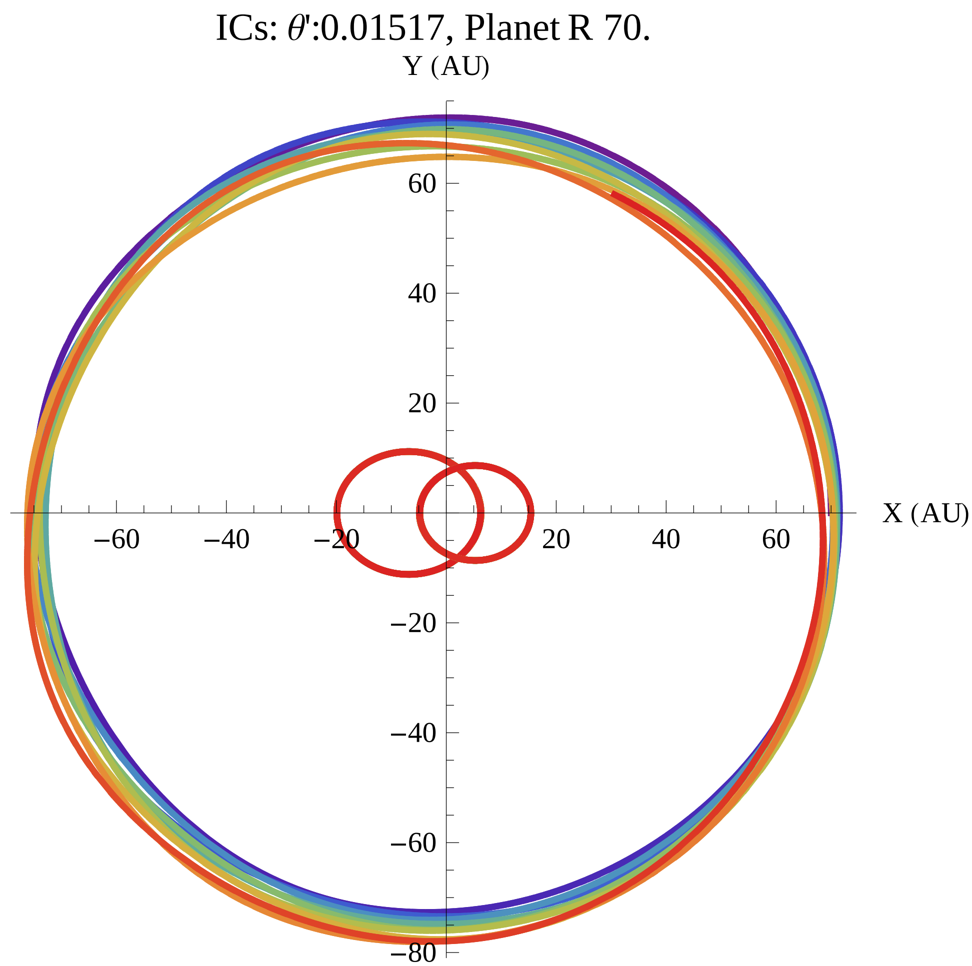

Figure 4: **P-Type Orbit** - The planet orbits both binary stars. The constantly-changing positions of the two inner stars cause small changes in the radius of the planet's orbit, but the orbit remains stable for over 7000 years. The actual orbit radii are very close to the predictions of a planet's radius about a single star with the mass of both binary stars if given the same initial conditions.

color maps linearly to time, a region of rapid color change is brought by low velocity, and slow color change by high velocity. All subsequent simulations follow this color convention.

The model predicts two different types of orbits for the planet's motion: the P-type orbit characterized by the planet orbiting both stars, and the S-type characterized by the planet orbiting only one of the stars. P-type orbits were found to be stable at large distances from the binary stars. At these distances, the two stars behavior can be approximated as a single star at the system's barycenter. Experimentation with various initial conditions that resulted in circular orbits yielded a closest stable orbit radius of ≈ 70 AU, very close to the single-star approximation radius of 69.4 AU. This orbit is shown in Fig. 4.

To generate an P-Type orbit, initial conditions requisite for a circular orbit with constant radius r of a planet of mass m around the total mass of the binary stars:

$$\frac{mv^2}{r} = \frac{mr^2\dot{\theta}^2}{r} = mr\dot{\theta}^2 = \frac{GMm}{r^2}$$

$$\dot{\theta} = \sqrt{\frac{GM}{r^3}} \tag{25}$$

where $M = M_1 + M_2$. Solving this equation for r yields the single-star approximation radius. At a close distance to the stars, like 70 AU, the planet's orbit is noticeably different from circular. Closer orbits become increasingly sensitive to the binary nature of the star system, and their orbits disintegrate more rapidly.

S-type planetary orbits occurred in the regions around each member of the binary. Stable orbits were found up to 5 AU away from the less massive star, as shown in Fig. 5, and up to 3 AU away from the more massive star.

The same basic process for generating stable P-type orbits can be used to generate stable S-type orbits. Rather than calculate the radius of the planet's travel around the barycenter, Eq. (25) is solved for the circular orbit radius about one of the stars. The M in Eq. (25) then represents the mass of the primary or secondary star. In addition, a second term must be added to this calculated angular velocity to account for the motion of the star. Thus, the only motion apparent in the star's center of mass frame is the desired circular orbit.

Of course, not all orbits conceived in this manner are stable due to the influence of the second star. Stability is tested for by giving the planet a small initial $\dot{r}$ in either direction and ensuring that the orbit approaches or oscillates about the same steady state radius. Orbits far away from their central star are increasingly affected by the other star. As expected, the smaller the radius of orbit, the less deviation from the ideal single-star circular orbit is observed. An example of a tight orbit is shown Fig. 6 to be contrasted with the large disturbances seen in Fig. 5.

The tight orbit is better understood when viewed in the frame of its parent star, as shown in Fig. 9. While the orbit is clearly elliptical, it is not wildly so, and its ellipticity can be seen to vary throughout the period of the binary, decreasing when the binary approaches apogee and increasing when the binary reaches perigee. In order to more clearly observe the dependence of the planet's motion on the star's motion, both the X and Y components of the planet's motion in the parent star's frame are plotted over several periods of the binary's orbit in figures Fig. 7 and Fig. 8 respectively.

The graphical results suggest that the radius' deviations are periodic with a period similar to the period of the binary system. A Fourier transform provides a way to further test this hypothesis. Taking the Fourier transform of the X component of the planet's orbital radius over a timescale that encompassed multiple 80-year periods yields the frequency domain analysis shown in Fig. 10.

In Fig. 10, the first independent peak corresponds to the orbital period of the planet around its parent star at 1.051 inverse years. This figure agrees with its observed rotation. More interesting however are the several smaller peaks that surround the primary one. These peaks can be more clearly observed in Fig. 11, which displays the Fourier analysis only in neighborhood of the peak of interest. The peaks on either side of the primary are exactly

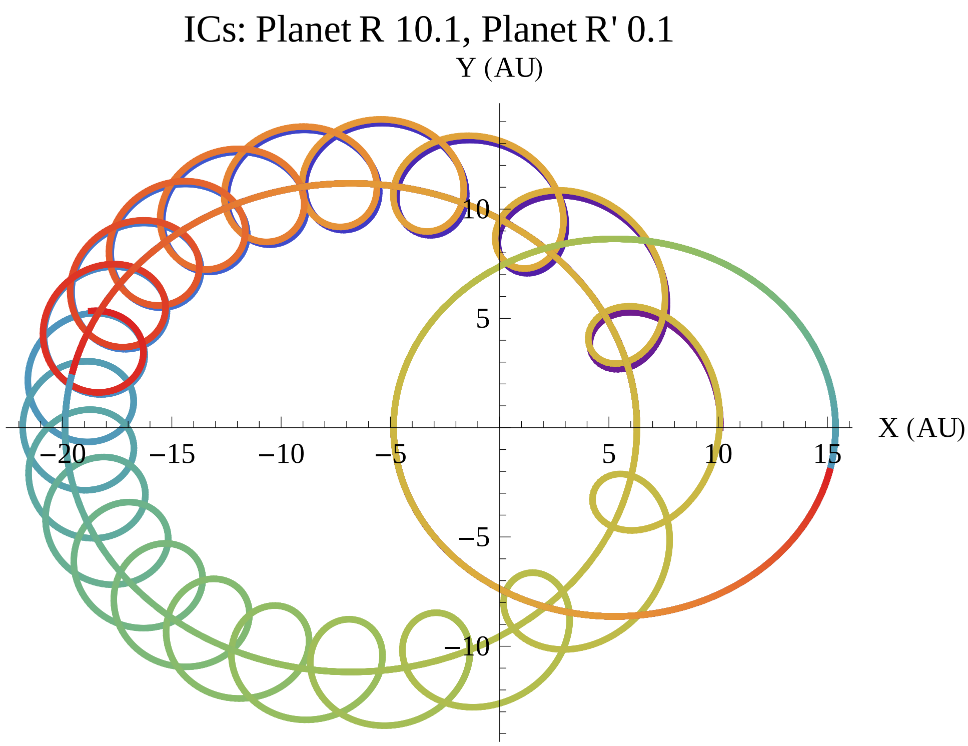

Figure 5: **S-Type Orbit** - A planet orbits one of the two binary stars. Notice how much the secondary star affects the planet's motion. The effect is most evident at the semi-major axis. Because the stars elliptical orbits return to the same position after 80 years, in a long simulation like this one, the stars overwrite their old positions. In this figure, neither star has a purple region because the orange region is on top of it.

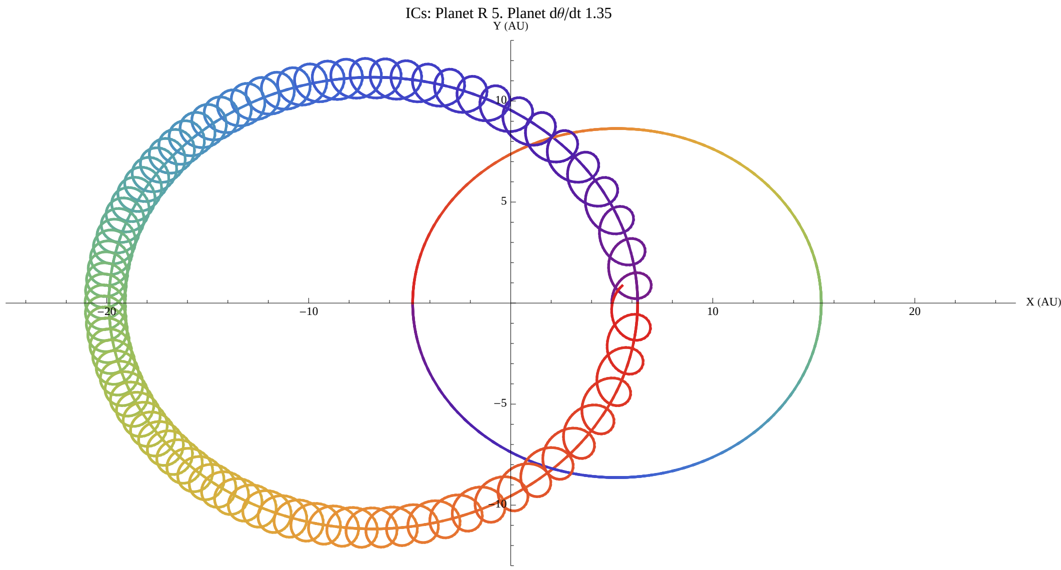

Figure 6: **A Tighter Orbit** - The closer the planet is to one of the two stars, the less affected it is by the other.

0.0125 inverse years away, and the spacing between all subsequent peaks is roughly the same value. 0.0125 inverse years is significant because it corresponds to an 80 year period, exactly that of the binary. Clearly this is evidence for some form of dependence on the binary orbit, though the nature of this dependence has not been determined. It should be noted that these contributions are very small compared to that of the planet's orbit, and can be left for future work.

While it was originally believed that these peaks were some residue of the Fourier analysis, the fact that the space between them exactly corresponded to the period of the binary suggests that they are not. In addition, experiments in varying both the sampling rate and sample size yielded no change in the structure or placement the peaks, leading to the conclusion that this phenomena must be physical.

In addition to S- and P-type orbits, interesting behavior was observed in unstable orbits when the planet was pulled too close to one star. This "collision" resulted in the planet's ejection from the system. Since our model approximates the planets and stars as points and does not conserve energy due to the massive approximation, a better model is necessary to gain intuition on planet ejection.

Unfortunately, the investigation into the existence of figure-eight planetary orbits around both stars was unsuccessful. Any such orbits, if they do exist, must be highly unstable and repulsive. While such analysis would be

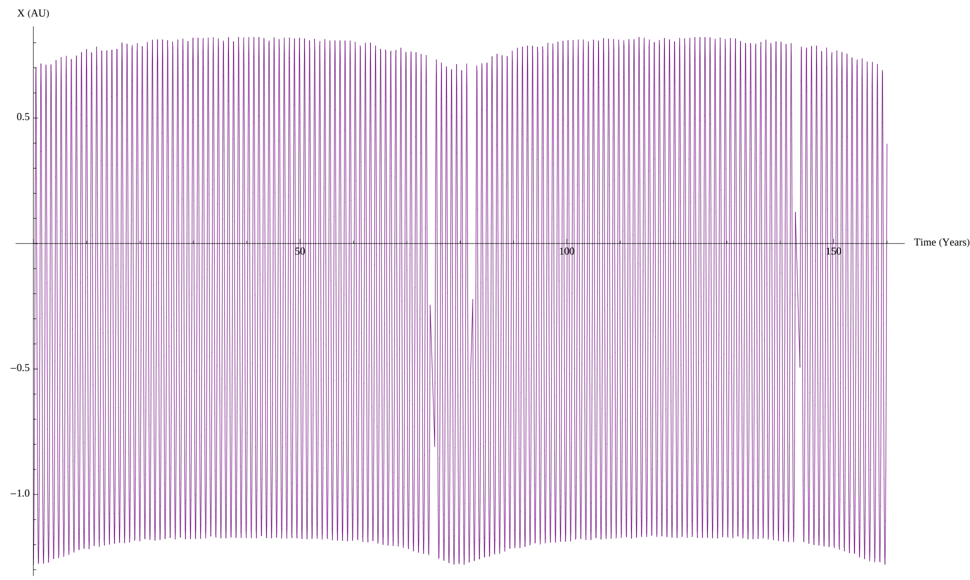

Figure 7: **X Planetary Motion in Parent Star's Frame** - X position of the planet in the center of mass frame over roughly two periods of the binary's orbit. Cyclic behavior with a period of 80 years is clearly observable.

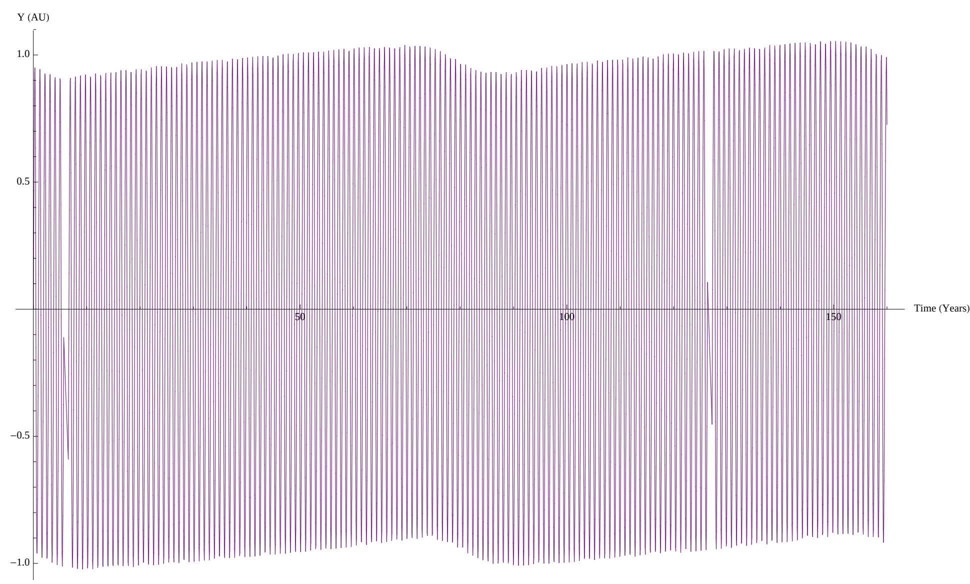

Figure 8: **Y Planetary Motion in Parent Star's Frame** - Y position of the planet in the center of mass frame over roughly two periods of the binary's orbit. Cyclic behavior with a period of 80 years is clearly observable.

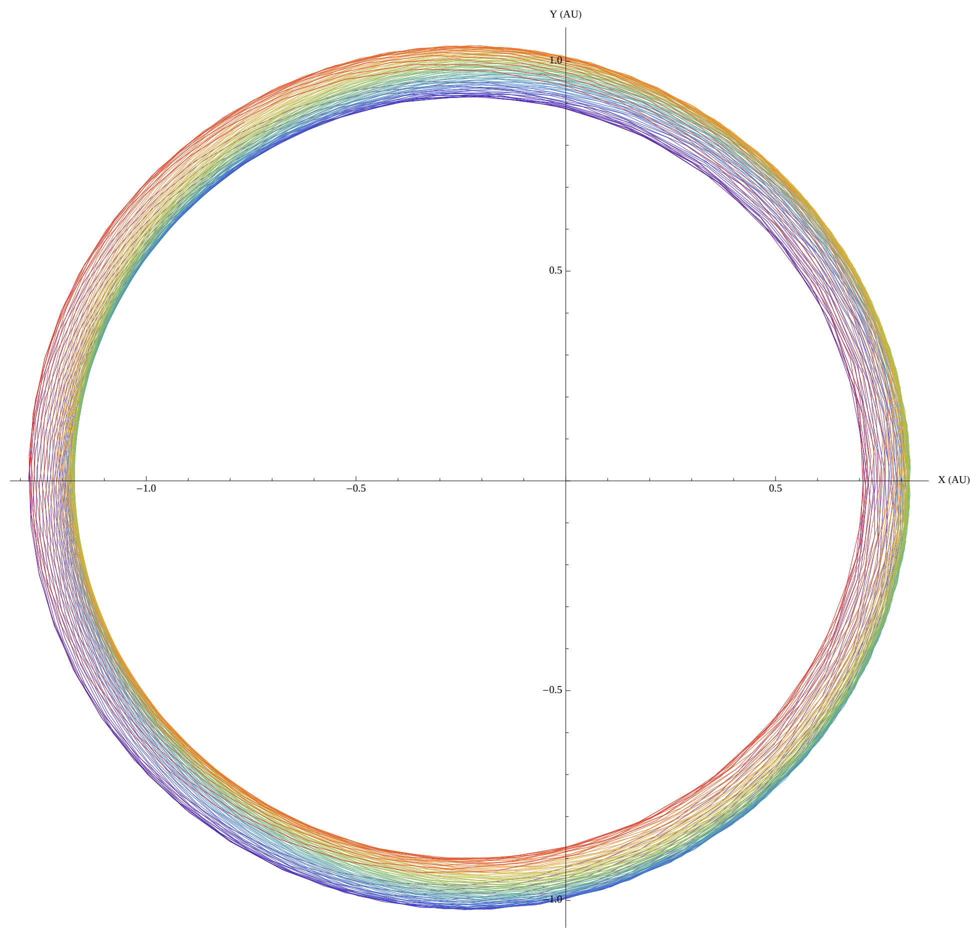

Figure 9: **Tight Orbit in Parent Star's Frame** - Orbiting around its parent star at the origin, the planet executes a nearly circular path. The ellipticity of its orbit becomes less as the binary orbit approaches apogee.

outside of the scope of this project, it would be interesting to calculate the Roche lobe analytically. Since the Roche lobe is a constant-energy surface shaped like a figure-eight, initial conditions that caused a planet to stay near this surface might yield such an orbit.

During the search, some interesting planetary orbits were discovered. One such orbit is P-type, but maintains a separation of roughly 5 AU from its parent star. As such, it is heavily influenced by the secondary star, as shown in Fig. 12; in fact, at its closest approach, the planet is nearly as close to the less massive secondary star as it is to the primary star. While this arrangement usually resulted in instability, this particular set of initial conditions results in a stable orbit for over 500 years. This may be due to a near-integral number of planet-star rotations ($\approx$7) for every star-star

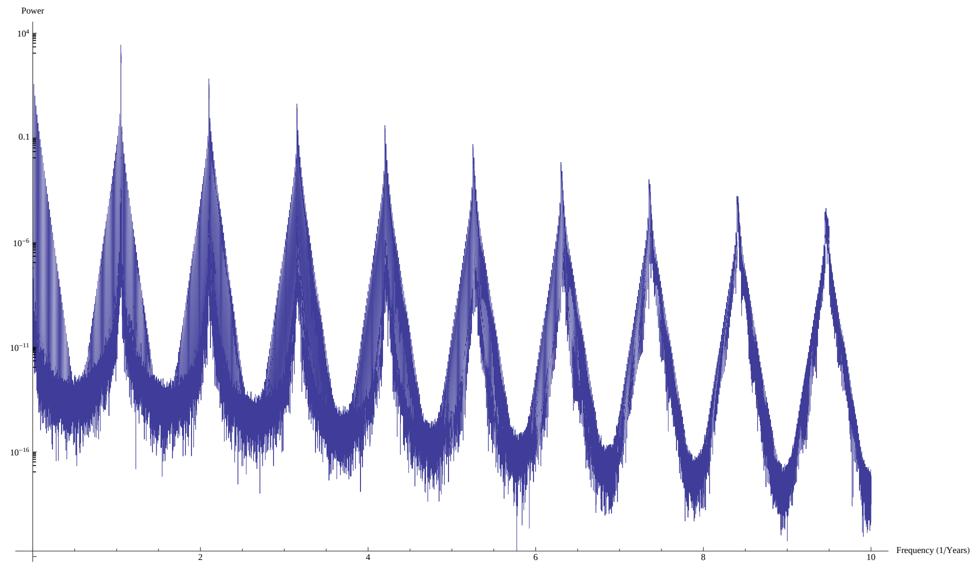

Figure 10: **Fourier Transform** - Fourier Transform sampling 10000 years of data at intervals of .05 years. A strong peak is observed at 1.051 inverse years corresponding to the orbit of the planet around its parent star.

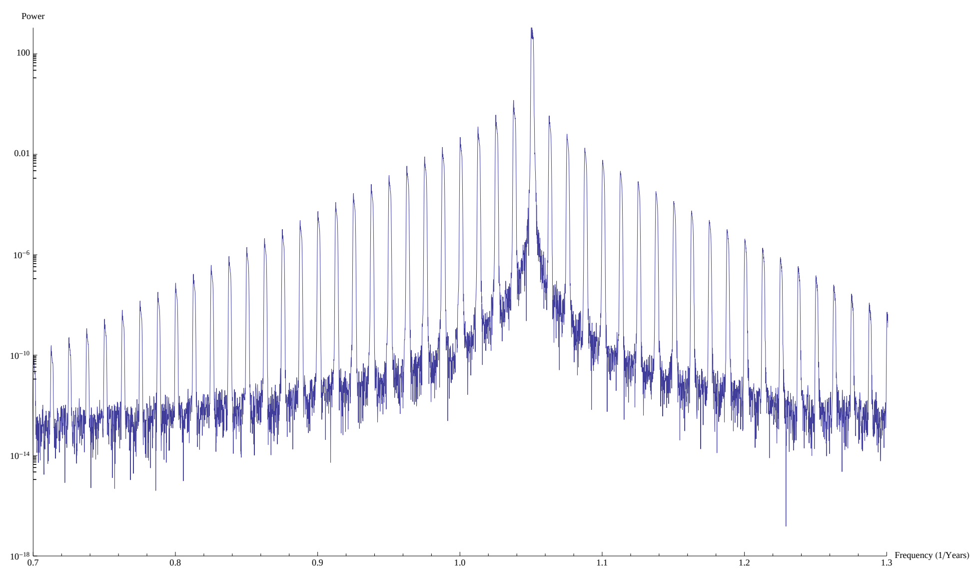

Figure 11: **Fourier Transform** - Fourier Transform sampling 10000 years of data at intervals of .05 years. The window is restricted to the region contain the strong peak observed in Fig. 10. Surrounding this peak are several evenly spaced peaks several orders of magnitude weaker than the central one. The spacing between the peaks was determined to be exactly .0125 inverse years, corresponding to a period of 80 years.

rotation.

A second area of interest was to ascertain the possibility of a planet switching from a P-type orbit around one star to a P-type orbit around the other. A more interesting orbit was found: the system in Fig. 13 started orbiting around the less massive star, switched to an orbit around the other star, and switched back to the first star. This system was not stable, because eventually the planet was ejected from the system or collided with one of the stars.

4 Conclusion

The restricted 3-body problem was successfully solved. The model predicts the existence of stable planetary orbits around binary stars, both of type S and P. Fourier analysis identified that the binary nature of the system resulted in small but measurable disturbances in both S and P type orbits.

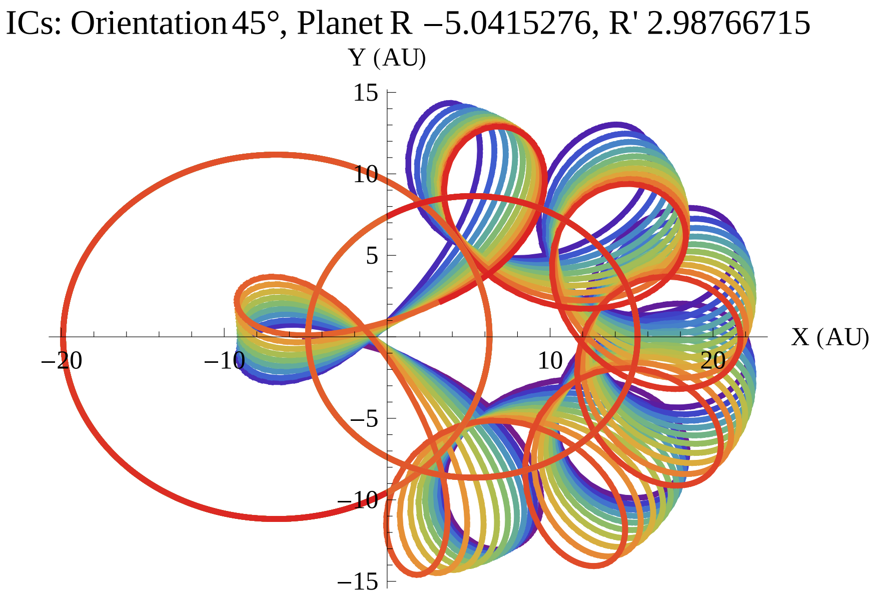

Figure 12: **Orbital Shifting** - A planet orbits one of the binary stars, but is influenced by the other. The frequency of its orbit around its star is close to, but not exactly, an integer multiple of the frequency of the binary star system, resulting in a gradual rotation of the planet's orbit over time.

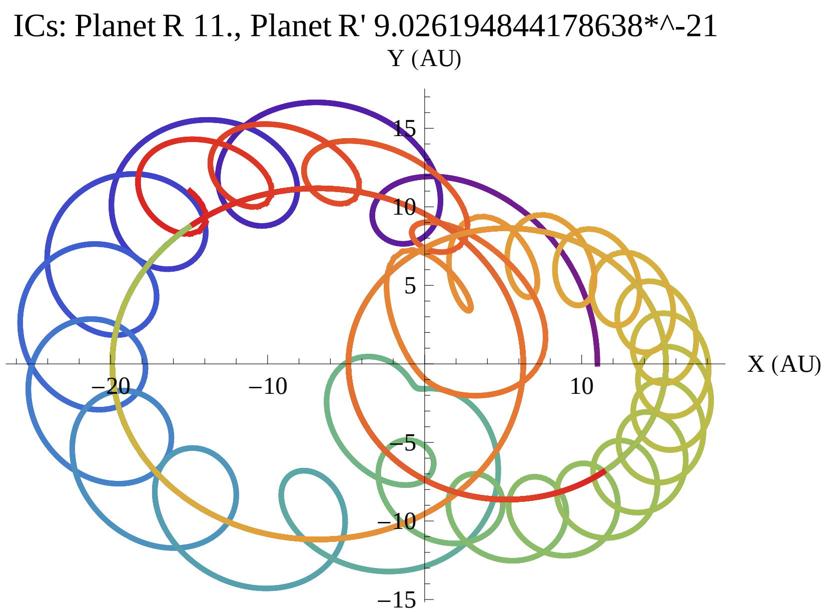

Figure 13: **Orbital Switching** - The planet starts orbiting one star, but switches to the other star and back again. Such a system is highly unstable and is not observed in nature.